Chapter 8
Modelling the Sea Ice Export Through Fram Strait

Torben Koenigk, Uwe Mikolajewicz, Helmuth Haak, and Johann Jungclaus

8.1 Introduction

The Arctic plays an important role in the climate system. The sea ice controls most of the heat, momentum and matter transfers in the ice-covered Arctic regions. Furthermore, melting and freezing of sea ice have a considerable impact on the ocean stratification. Only a small fraction of the salt is included in the sea ice during freezing processes while the majority is released to the underlying ocean layer. The density of the seawater is increased, which may lead to a destabilization of the ocean stratification. In contrast, melting of sea ice represents a freshwater input into the ocean. The density is reduced and the ocean stratification stabilized. It is of great importance for the ocean where sea ice is freezing and melting. The formation area is not necessarily the same as the melting area. The transport of ice along with the associated freshwater and negative latent heat plays a critical role in the climate system.

The largest sea ice export out of the Arctic Ocean takes place through Fram Strait. It represents a very important flux of freshwater into the North Atlantic Ocean. After passing Fram Strait, the sea ice/freshwater propagates along the east coast of Greenland to the south and into the Labrador Sea. Dickson et al. (1988) and Belkin et al. (1998) suggested that the Great Salinity Anomaly (GSA) observed in the Labrador Sea in the early 1970s was caused by previous large positive ice export anomalies through Fram Strait. Häkkinen (1999) simulated this process by prescribing idealized freshwater pulses in the East Greenland Current in an ocean model. The observed salinity anomalies and the decrease in the oceanic convection were reproduced. Haak et al. (2003) concluded, from simulations with the ocean model MPI-OM that the GSA's in the 1980s and 1990s were caused by anomalous large ice export events through Fram Strait as well.

In a recent paper, Koenigk et al. (2006) showed with a global coupled atmosphere–ocean model that large ice export events through Fram Strait have a significant impact on the atmosphere. The reduced convection in the Labrador Sea after positive ice export anomalies leads to colder ocean surface temperatures, an increased ice cover and consequently a reduced ocean heat release to the atmosphere. Air temperature in the

Max-Planck-Institut für Meteorologie, Bundesstraβe 53, 20146 Hamburg, Germany

R.R. Dickson et al. (eds.), *Arctic–Subarctic Ocean Fluxes*, 171–191

Labrador Sea is therefore significantly reduced and large-scale atmospheric circulation is influenced 1 and 2 years after high ice exports through Fram Strait. Based on these results, Koenigk et al. (2006) suggested a high predictive skill for atmospheric and oceanic climate in the Labrador Sea.

Variations of the ice export through Fram Strait have a considerable effect on ice cover in the Greenland Sea (Walsh and Chapman 1990) and can lead to large and long lasting anomalies. Observational analysis of Deser et al. (2000) suggested a northward shift in the storm track as a consequence of low ice concentration in the Greenland Sea. They argued that SLP in the Greenland Sea is decreased due to enhanced heat fluxes from ocean to atmosphere in areas of reduced sea ice. In contrast, model results of Magnusdottir et al. (2004) and Deser et al. (2004) showed a negative NAO pattern as response to reduced sea ice cover in the Greenland and Barents Sea.

Observations in the Arctic are rather sparse and exist only for the last decades, which were characterized by an unusual state of the general atmospheric circulation and large trends in Arctic climate parameters. Hence, in this study, a 500-year control integration of the global coupled atmosphere–ocean–sea ice model ECHAM5.0/MPI-OM is used to analyze the ice export through Fram Strait and its interannual to decadal variability. The length of the integration provides the possibility to perform statistical analyses on different time scales. The results are compared both with observational data and other model studies.

8.2 Model Description

The model used in this study is the Max-Planck-Institute for Meteorology's global coupled atmosphere–ocean–sea ice model ECHAM5.0/MPI-OM. It consists of the fifth cycle of the atmosphere model ECHAM (ECmwf HAMburg) and the ocean model MPI-OM (Max-Planck-Institute Ocean Model). The atmosphere model ECHAM5.0 (Roeckner et al. 2003) is run at T42 resolution, which corresponds to a horizontal resolution of about 2.8° × 2.8°. It has 19 vertical levels up to 10 hPa. The ocean model MPI-OM (Marsland et al. 2003) includes a Hibler-type dynamic-thermodynamic sea ice model. The grid has a resolution of about 2.8° but with an increasing refinement of the meridional grid spaces between 30° N to 30° S up to 0.5° from 10° N to 10° S. The North Pole is shifted towards Greenland (30° W, 80° N) to avoid the grid singularity at the geographical North Pole. Thus, the model resolution in Fram Strait and the deep convection areas of Greenland and Labrador Sea is relatively high. The model's South Pole is located at 30° W, 80° S.

The atmosphere and the sea ice–ocean model are coupled by the OASIS coupler (Valcke et al. 2003). The coupler transfers fluxes of momentum, heat, and freshwater from the atmosphere to the ocean and sea surface temperature and sea ice properties from the ocean to the atmosphere. The climate model includes a river runoff scheme (Hagemann and Düemenil 1998, 2003). Glacier calving is included in a way, that the amount of snow falling on Greenland and Antarctica is instantaneously transferred into the nearest ocean point. In the coupled model no flux adjustment is used.

A 500-year control integration from this model has been used in this study. Analyses of multidecadal scale changes in the North Atlantic thermohaline circulation by Latif et al. (2004) and analyses of the impacts of the Fram Strait ice export on climate by Koenigk et al. (2006) are based on the same control integration.

8.3 Results

8.3.1 Mean Sea Ice Export Through Fram Strait

Above, we discussed the importance of the Fram Strait sea ice export for the climate system. Table 8.1 shows observation-based estimates and parameterizations of the ice export from different studies. Aagaard and Carmack (1989) used ice volume flux measurements from moored upward looking sonars (ULS) by Vinje and Finnekåsa (1986) at 81° N and results from Untersteiner (1988) to estimate the Fram Strait ice export. They found a mean export of about 100,000 m^3/s. Vinje et al. (1998) used ULS to obtain the ice thickness at 79° N for the time period 1990–1996. Together with the velocity, derived from the cross-strait sea level pressure (SLP) gradient, they calculated the ice export through Fram Strait. The mean of the 7-year period was 83,000 m^3/s. Annual mean values vary substantially between about 60,000 m^3/s and 150,000 m^3/s. The export is largest in March with slightly below 120,000 m^3/s and smallest in August with about 40,000 m^3/s. They determined an error for monthly measurements of 8–17% for ice area flux and about 0.1 m for ice thickness. This amounts to an error of approximately 12% for the highest and 20% for the smallest monthly fluxes. Vinje (2001) parameterized the ice export through Fram Strait for the period 1950–2000 by using the close relationship between the SLP gradient across Fram Strait and the ice export. The mean export of the 50-year period was 92,000 m^3/s with a standard deviation of about 21,000 m^3/s. Schmith and Hansen (2003) used sea ice observations from the southwest coast of Greenland to reconstruct the ice export through Fram Strait. The extent of the summer sea ice depends on the ice export through Fram Strait in the previous winter. The authors found an average ice export of 100,000 m^3/s and both a strong interannual variability and a marked multi-decadal variability

Table 8.1 Observation-based estimates of the mean sea ice export through Fram Strait in m^3/s

Author	Time	Ice export (m^3/s)
Aagaard and Carmack (1989)	1953–1984	100,000
Vinje et al. (1998)	1990–1996	83,000
Vinje (2001)	1950–2000	92,000
Schmith and Hansen (2003)	1820–2000	100,000
Kwok et al. (2004)	1991–1998	70,000

with low ice exports around 1920/1930 and high exports in the 1950s and 1960s. Kwok et al. (2004) used ULS data from 1991 to 1998 and found a mean ice export through Fram Strait of 70,000 m^3/s with a standard deviation of approximately 15,000 m^3/s. The authors indicated that 50% of the ice export takes place during December and March while the summer export is weak. It has to be noted that both the mean export and the standard deviation is substantially smaller in Kwok et al. (2004) than in Vinje et al. (1998) although the same ULS data and almost the same time period has been used. Kwok et al. (2004) derived the ice motion from satellite passive microwave data while Vinje et al. (1998) used the SLP gradient across Fram Strait to estimate the ice velocity.

Table 8.2 summarizes model simulations of the Fram Strait ice export. Häkkinen (1993) used an ocean–sea ice model for the Arctic and the northern North Atlantic, forced with monthly means of NCEP/NCAR-reanalysis data (Kalnay et al. 1996). The ice export is relatively small with 63,000 m^3/s because ice thickness is slightly underestimated in the model. Simulations with sea ice models (Hilmer et al. 1998; Arfeuille et al. 2000) and ocean–sea ice models (Koeberle and Gerdes 2003; Haak et al. 2003), forced by 40- or 50-year reanalysis data, all indicate a high interannual to decadal variability. All model simulations show pronounced ice export events in 1967/68 and in 1994/95. The mean exports are similar (83,000–104,000 m^3/s), except for the model of Arfeuille et al. (2000) that simulated an average ice export of 160,000 m^3/s. Nevertheless, their ice export anomalies compare well with the other model simulations.

In this study, a global coupled atmosphere–ocean–sea ice model is used. Hence, only statistics of the time series (Fig. 8.1a) can be compared to observations and other studies. The mean export amounts to 97,000 m^3/s, which is in the upper range of observation-based estimates and model simulations. The ice export is highly variable on interannual time scales with a standard deviation of 21,000 m^3/s for annual mean exports. The monthly mean ice export through Fram Strait, averaged over the 500-year control integration (Fig. 8.1b), shows a pronounced seasonal cycle. The maximum occurs in March with an average of 147,000 m^3/s and the minimum in August with 35,000 m^3/s. This agrees with observation-based estimates by Vinje et al. (1998) and parameterizations by Vinje (2001). The standard deviation has been calculated for each month.

Table 8.2 Model simulations of the mean sea ice export through Fram Strait in m^3/s

Author	Time	Ice export (m^3/s)
Häkkinen (1993)	1955–1975	63,000
Hilmer et al. (1998)	1958–1997	91,000
Arfeuille et al. (2000)	1958–1998	160,000
Koeberle and Gerdes (2003)	1948–1998	83,000
Haak et al. (2003)	1948–2001	104,000
Koenigk et al. (2006)	500-year ctrl-run	97,000

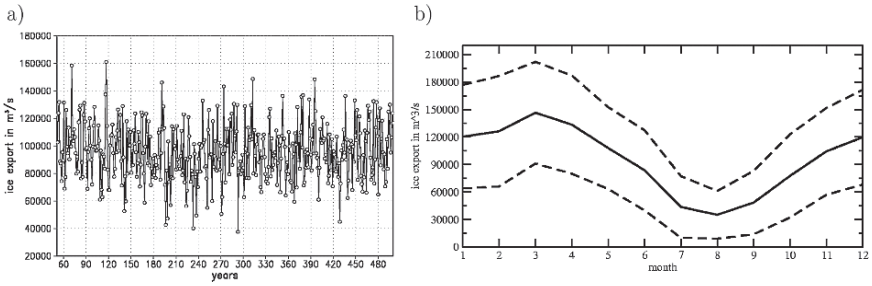

Fig. 8.1 (a) Annual mean ice export through Fram Strait in m^3/s. (b) Monthly mean ice export (solid) and ice export ± 1 standard deviation (dashed) in m^3/s, averaged over the 500-year control integration for each month

Table 8.3 Correlation between seasonal mean ice exports through Fram Strait. Seasons, written in the horizontal, lead seasons, written in the vertical. The last row indicates the correlation between the annual mean ice export (averaged from September to August) and the single seasons

	DJF	MAM	JJA	SON
DJF	1	0.34	0.10	0.04
MAM	–0.04	1	0.15	0.14
JJA	0.12	0.01	1	0.31
SON	0.25	0.00	0.11	1
Year	0.75	0.64	0.50	0.57

It is largest in late winter/early spring with 50,000–60,000 m^3/s, but even in late summer it amounts to more than half of the winter values and contributes considerably to the interannual variability. Hence, the ice export in late summer/early autumn should not be neglected.

The correlation among single seasons is presented in Table 8.3 Sequenced seasons are weakly positively correlated with coefficients between 0.15 for spring (MAM) – summer (JJA) and 0.34 for winter (DJF) – spring (MAM). The correlation between non-sequenced seasons is very low. All seasons are significantly and highly positively correlated with the annual mean ice export. The correlation is largest in winter but still reaches 0.5 and 0.57 in summer and autumn, respectively.

The same correlation analysis is performed for ice exports of single months. Sequenced months are significantly positively correlated, whereas highest correlations occur between July–August ($r = 0.41$), August–September ($r = 0.42$) and September–October ($r = 0.41$) ice exports. In this time period, during summer and early autumn, wind variability is much weaker than in winter and the ice export depends largely on the amount of ice remaining from the previous winter.

8.3.2 Variability of Sea Ice Export

As shown above, the interannual to decadal variability of the ice export through Fram Strait is very high. Figure 8.2 shows the energy spectrum of annual mean ice exports through Fram Strait in the 500-year integration of our model. Three peaks in the ice export at time scales of about 3–4 years, 9 years and 15 years can be observed.

These three peaks, although shifted towards slightly shorter time scales, can be found in the reconstructed ice export time series of Schmith and Hansen (2003). Several other studies (e.g. Venegas and Mysak 2000; Hilmer and Lemke 2000; Polyakov and Johnson 2000) also found peaks at roughly 10 years in Fram Strait ice export and Arctic atmospheric circulation regimes. Venegas and Mysak (2000) and Goosse et al. (2002) reported significant variability in the Arctic ice volume at a timescale of 15–20 years, which might fit to the 15-year peak in the ice export in this study.

The interannual variability of the Fram Strait ice export is highly related to the local wind forcing. Figure 8.3a presents a correlation analysis between annual mean ice exports through Fram Strait and SLP anomalies in our model simulations. In the area of the Kara Sea, correlation exceeds –0.6. A smaller positive correlation exists over the Canadian Archipelago. This pattern is related to anomalous winds from the coasts of Laptev, East Siberian, Chukchi and Beaufort Seas across the Arctic towards Fram Strait and enhanced northerly wind stress in Fram Strait. Consequently, ice is anomalously transported towards Fram Strait in the entire Arctic Basin (Fig. 8.3b). The correlation between annual mean ice export and SLP gradient across Fram Strait is 0.86. The SLP gradient explains therefore about three quarters of the annual mean ice export variability. This is in agreement

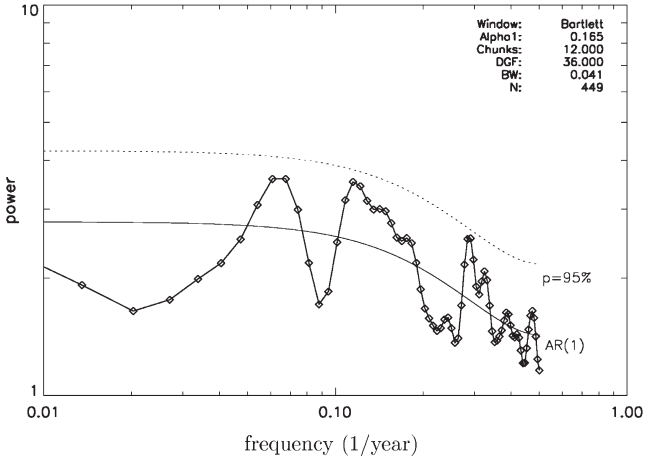

Fig. 8.2 Spectral analysis of annual mean Fram Strait ice export (Based on Koenigk et al. 2006)

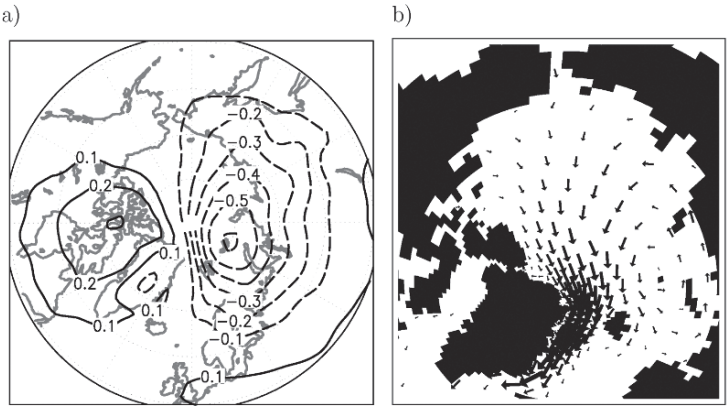

Fig. 8.3 (a) Correlation pattern between annual mean ice export through Fram Strait and sea level pressure. (b) Regression pattern between Fram Strait ice export and sea ice transport in the Arctic. The areas of the arrows show the amount of ice transport. The smallest arrow shown represents an ice transport of 0.1×10^{-2} m^3/s per standard deviation ice export, the largest 6.3×10^{-2} m^3/s. Each 16th arrow is shown (Based on Koenigk et al. 2006)

with observation-based estimates of Kwok and Rothrock (1999) who found an explained variance of 80%.

8.3.2.1 North Atlantic Oscillation

The North Atlantic Oscillation (NAO, Hurrel and van Loon 1997; Bojariu and Gimeno 2003) governs important parts of climate variability in high northern latitudes. However, its impact on the ice export through Fram Strait is still under debate. Kwok and Rothrock (1999) found a correlation coefficient of 0.86 for the period 1978–1998. Simulations with a sea ice model (Hilmer and Jung 2000) indicated similar results for this time period but no significant correlation between ice export and NAO before 1978. Analysis of a 300-year control run of the atmosphere–ocean–sea ice model ECHAM4/OPYC3 by Jung and Hilmer (2001) showed no significant correlation either. The changing character of the relation between ice export and NAO can be explained by an eastward shift in the extension of the Icelandic Low into the Arctic since the late 1970s. This shift leads to an increased pressure gradient across Fram Strait in the positive NAO case. Before 1978, the NAO did not affect the SLP gradient across Fram Strait at all. Whether the shift in the Icelandic Low is due to anthropogenic climate changes or natural variability cannot yet be determined. Ostermeier and Wallace (2003) analyzed the trends in the NAO over the 20th century. They found a negative trend from 1920 to 1970 and a strong positive trend since. In our model simulations, the NAO has neither influenced the ice volume export through Fram Strait nor the pressure gradient across Fram Strait. Nevertheless, the anomalous SLP pattern and the associated

wind anomalies lead to strong anomalous ice transports from the Barents Sea across the North Pole to the Beaufort Sea. Ice transport to the south is enhanced in the Baffin Bay and in the Labrador Sea (not shown).

To elucidate the temporal relationship between NAO-index and sea ice export through Fram Strait, running 30-year intervals of the 500-year control run are analyzed (not shown). In the entire 500 years, not a single 30-year period with a high correlation between NAO and ice export or SLP gradient can be found. As no anthropogenic forcing is used in the model, this supports the presumption of Jung and Hilmer (2001) that the recent state of the NAO may be a response to anthropogenic forcing.

8.3.2.2 Stratospheric Polar Vortex

Several studies have recently discussed the effect of the stratospheric circulation on tropospheric climate. Christiansen (2001) as well as Graversen and Christiansen (2003) showed that zonal wind anomalies from the stratosphere propagate downward to the troposphere in about 10–15 days. Thompson et al. (2002) and Baldwin et al. (2003) proposed an increased skill from the stratospheric circulation to predict northern hemisphere tropospheric conditions on this time scale. Norton (2002) performed sensitivity experiments with an atmospheric general circulation model and altered the mean state and variability of the stratosphere. The wintertime SLP responded with a lag of 10–25 days with a pattern that is similar to the AO-pattern.

In this study, the impact of the stratospheric polar vortex on the ice transport in the Arctic and especially the ice export through Fram Strait is analyzed with ECHAM5/MPI-OM. The polar vortex index has been defined, according to Castanheira and Graf (2003), as the zonal mean zonal wind speed in 50 hPa height and 65° N.

In contrast to the NAO, the annual mean stratospheric polar vortex index is significantly positively correlated ($r = 0.34$) with the annual mean ice export through Fram Strait in the control integration although the explained variance is rather small.

Figure 8.4a displays the difference of annual mean SLP between strong and weak stratospheric polar vortex regimes (exceeding the mean ± 1 standard deviation). The largest differences occur over the Barents Sea with more than −2 hPa. Smaller positive values appear over the North Atlantic, Western Europe and the Bering Strait. This SLP pattern compares well with results of the sensitivity experiments of Norton (2002). The maximum pressure anomaly in ECHAM5/MPI-OM is slightly shifted towards the Barents Sea. It should be noted that annual mean values are used in this study while Norton focused on winter means.

The SLP anomalies lead to an increased SLP gradient across Fram Strait and stronger northerly winds during a strong polar vortex regime. The ice export through Fram Strait is consequently enhanced and vice versa during weak vortex regimes (Fig. 8.4b).

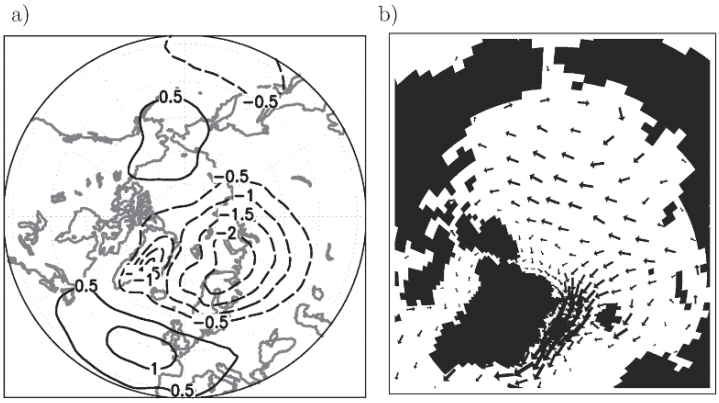

Fig. 8.4 Annual differences between strong and weak stratospheric polar vortex regimes: (a) SLP in hPa; (b) sea ice volume transport. The areas of the arrows show the amount of ice transport. The smallest shown arrow presents an ice export of 0.1×10^{-2} m^3/s per standard deviation ice export, the largest 5.2×10^{-2} m^3/s. Each 16th arrow is shown

8.3.2.3 Atmospheric Planetary Waves

Large-scale atmospheric planetary waves in the northern hemisphere are mainly caused by the topography and land–sea distribution (O'Hanlon 2002). Cavalieri and Häkkinen (2001) investigated the relationship between atmospheric planetary waves and Arctic climate variability. They performed a zonal Fourier analysis over a monthly averaged 50-year SLP-record from 1946 to 1995 for different latitude bands. They showed that the phase of the first wave for the latitude band from 70° to 80° N in January is well correlated with the ice export through Fram Strait. The Siberian High and the Icelandic Low determine the first wave. A ridge of the Siberian High that extends into the East Siberian and Chukchi Seas and a trough of the Icelandic Low into the Arctic form maximum and minimum of the first wave. A shift in the positions of the pressure systems to the east is associated with reduced pressure in the Barents and Kara Seas. Hence, the pressure gradient across Fram Strait is increased. In contrast to the NAO, the high correlation between ice export and the first wave in January held for the entire 50-year period. Cavalieri (2002) attributes this consistency to the sensitivity of the first wave phase to the presence of secondary low pressure systems in the Barents Sea that serve to drive Arctic sea ice southward through Fram Strait. Figure 8.5 shows the relation between sea ice export and first wave in the ocean–sea ice model MPI-OM (Haak 2004) forced by NCEP/NCAR-reanalyses. The correlation of both time series exceeds 0.6 considering the period 1948–2002. The interannual variability of the wave-1 phase seems to be related to the cyclonic and anti-cyclonic regimes proposed by Proshutinsky and Johnson (1997).

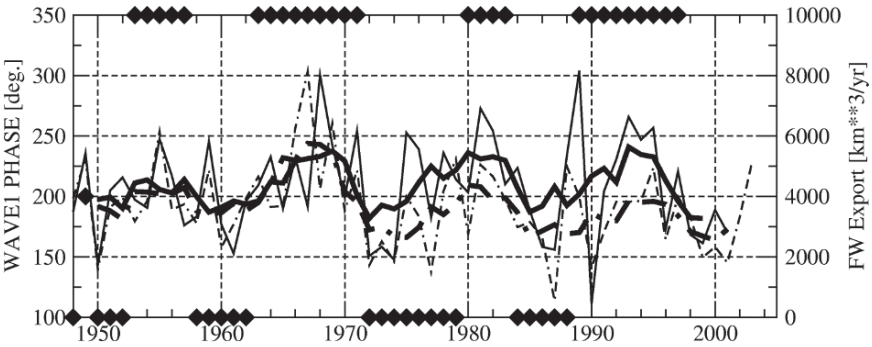

Fig. 8.5 Fram Strait solid freshwater export (solid) and phase of zonal SLP-wave-1 in 70–80° N (dashed) for January (taken from Haak 2004). Thick lines are smoothed by a 5-year running average. Black squares indicate the cyclonic (top) and anti-cyclonic (bottom) Arctic circulation regimes described by Proshutinsky and Johnson (1997). Units are (km^3/year) and (° lon.), respectively

In this study, the relationship suggested by Cavalieri and Häkkinen (2001) has been analyzed in the 500-year control integration. In accordance with their results, the ice export through Fram Strait is highly correlated with the phase of the first SLP wave for the latitude band from 70° to 80° N. This relation holds for the entire year but is highest in winter (r = 0.6 in February) while the correlation is quite weak in June and July (r = 0.2 resp. 0.15, Table 8.4). Annual mean values are correlated with 0.59.

In spite of the high correlation between phase and ice export, usage of the phase as index has some disadvantages. In months with small amplitude, the first wave explains only a minor part of the SLP variability and the phase is of minor importance. Furthermore, it is difficult to qualify large shifts in the phase as positive or negative because phase anomalies of nearly –180° or 180° both describe the same SLP pattern. A shift in the phase exceeding 90° is not further increasing the SLP gradient across Fram Strait and the ice export is not enhanced anymore. To avoid these difficulties, a new index containing both the phase and the amplitude of the wave is introduced here:

$$WI1 = A \cdot \sin(\Phi')$$

We call this index wave index 1 (WI1). A is the amplitude of the first wave and Φ′the phase anomaly. Use of sin(Φ′) instead of the phase anomaly has two effects: WI1 is decreased if the phase anomaly exceeds 90° and the function is continuously differentiable at the location Φ′ = 180°. Φ′ is weighted with the amplitude to reduce the noise of years with small explained variances of the first SLP wave. Table 8.4 displays the correlation between monthly mean WI1 and monthly mean ice exports through Fram Strait. The correlation is generally high between September and May with a maximum of 0.7 in February. It exceeds the correlation between wave phase and Fram Strait ice export in all months. During summer,

Table 8.4 Correlation between monthly means of the phase of wave number 1 and Fram Strait ice export (FP), WI1 and Fram Strait ice export (FI) and WI1 and SLP gradient across Fram Strait (FG)

	Jan.	Feb.	Mar.	Apr.	May	June	July	Aug.	Sept.	Oct.	Nov.	Dec.
FP	0.45	0.60	0.45	0.43	0.40	0.20	0.15	0.29	0.35	0.38	0.37	0.40
FI	0.66	0.70	0.61	0.66	0.59	0.34	0.26	0.35	0.49	0.54	0.56	0.59
FG	0.73	0.73	0.69	0.67	0.59	0.31	0.31	0.53	0.66	0.67	0.60	0.61

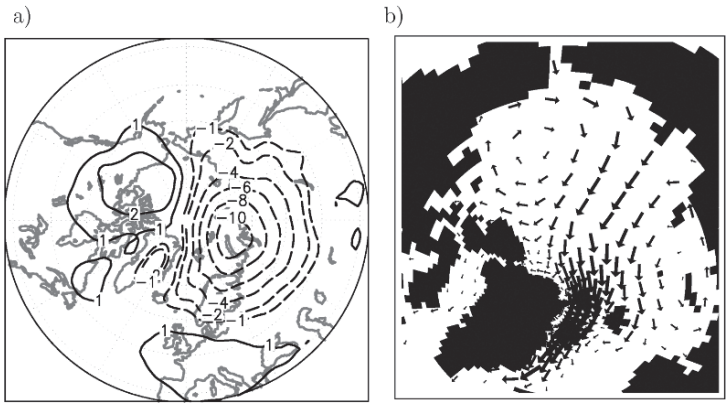

Fig. 8.6 Differences between high and low annual WI1 for (a) winter SLP in hPa, (b) annual sea ice thickness transport. The areas of the arrows show the amount of ice transport. The smallest arrow shown represents an ice export of 0.2×10^{-2} m^3/s per standard deviation ice export, the largest 12×10^{-2} m^3/s. Each 16th arrow is shown

correlation is significant but does not exceed 0.35. For comparison, the relation between WI1 and SLP gradient across Fram Strait is shown. This correlation is reduced in summer as well.

Figure 8.6a shows the SLP difference pattern between large positive and negative WI1 (exceeding the mean ± 1 standard deviation) for winter means. The pattern is characterized by negative anomalies of up to −10 hPa at the Siberian coast centered in the Kara Sea and much smaller positive anomalies of about 2 hPa in the western Arctic and in Western Europe. Obviously, the WI1 is mainly governed by SLP variations in the Kara Sea. This results in a steepened SLP gradient across Fram Strait during a positive WI1 and vice versa. Dorn et al. (2000) depicted from simulations with a regional coupled model that warm and cold Arctic winters are connected with two distinct circulation states of the Arctic atmosphere. Cold Januaries are characterized by the extension of the Icelandic Low into Barents and Kara Sea while warm Januaries are linked to a more pronounced Siberian High. These two states fit well to the WI1 pattern.

The associated large SLP anomalies affect the ice transport in the entire Arctic. Figure 8.6b displays the annual mean ice transport differences between positive and

Table 8.5 Correlation between DJF ice transport divergence in the Arctic regions and WI1

	Ba	Ka	La	Sib	Chu	Bea	CA	AB
WI1	−0.45	0.20	0.67	0.61	0.60	0.24	−0.75	0.57

Ba = Barents Sea, Ka = Kara Sea, La = Laptev Sea, Sib = East Siberian Sea, Chu = Chukchi Sea, Bea = Beaufort Sea, CA = Central Arctic, AB = Arctic Basin

negative WI1 (mean ± 1 standard deviation). Sea ice is anomously advected from the Siberian coast over the Central Arctic towards Fram Strait and Barents Sea. In the Beaufort Gyre a weak anticyclonic circulation occurs. Ice transport differences are largest in Fram Strait and East Greenland Current where they reach 0.1 m^2/s. The probability distribution of annual mean ice exports through Fram Strait for highly anomalous WI1 (not shown) provides evidence that almost all extreme export events in the 500-year control run are related to WI1. The distributions for the cases of large positive and negative WI1 show a distinct shift towards corresponding positive and negative ice export anomalies.

The composite patterns for SLP and ice transport resemble the correlation and regression patterns between ice export through Fram Strait and SLP and ice transport, respectively (Fig. 8.3). The ice transport anomalies due to the WI1-variability are associated with variations in the ice transport divergence (Table 8.5). During positive WI1, ice transports diverge anomalously from the Laptev Sea to the Chukchi Sea. Ice transports converge in the Barents Sea and particularly in the Central Arctic. The entire Arctic shows a loss of ice volume due to the large ice export through Fram Strait.

It has been demonstrated above that the state of the WI1 is mainly characterized by the SLP in the Kara Sea. The persistence and the source of these SLP anomalies are analyzed below.

The correlations among consecutive months of WI1 are very weak. The highest correlation coefficient of 0.15 is obtained between WI1 of January and February. Furthermore, daily winter (DJF) SLP values in the Kara Sea are compared for months with high positive and negative WI1. Two features are particularly striking: The SLP for positive WI1 in the Kara Sea is generally lower than for negative WI1 and the variability is larger. A sequence of short, relatively large negative anomalies occurs during positive WI1. Contrary, high SLP can persist for a time of 1–2 weeks in the Kara Sea during a negative WI1. During a positive WI1, more cyclones are active in the Barents and Kara Seas while in the negative case, longer periods with stable anticyclonic regimes occur.

Storm tracks are calculated from daily winter SLP data to determine the cyclonic activity. In this study, the standard deviation of the 2–6 days band-pass filtered daily SLP data is defined as storm track (Blackmon 1976). A composite analysis of these storm tracks for winter means of the WI1 (Fig. 8.7) shows distinct differences between the phases of WI1. During positive WI1, the storm track over the North Atlantic extends far into Barents and Kara Sea, whereas it is much more zonal

during negative WI1 and the standard deviation of the band-pass filtered daily SLP in the Barents and Kara Seas is small. The standard deviation in the formation area of the North Atlantic low-pressure systems over northeastern North America is slightly increased in the positive WI1 case. Thus, an intensification of the North Atlantic storm track and especially a deflection to the north are the main reasons for a positive WI1. The cyclones propagate mainly from the North Atlantic into the Barents and Kara Sea and are not formed locally. This is in agreement with results of Serreze and Barry (1988). They analyzed the winter synoptic activity in the Arctic Basin and found the largest activity in the European sector of the Arctic. Most of the cyclones migrated from the North Atlantic into the Arctic. As the Fram Strait is located on the western side of the storm track, an enhanced pressure gradient across it and anomalously northerly winds are the consequence. This implies that single cyclones are of great importance for the ice export through Fram Strait, which fits well to observations of cyclones in the Fram Strait by Brümmer et al. (2001, 2003).

During a negative WI1 the Siberian High extends further into the Kara and Barents Seas and the storm track is more zonal. It remains unclear whether the Siberian High can extend further to the northwest due to a weaker, more zonal storm track or if a strong Siberian High blocks the cyclones. One possible mechanism affecting the Siberian High may be related to snow anomalies over Siberia in early fall. Cohen et al. (2000) showed that they influence SLP in the northern hemisphere and affect the AO in the following winter. Gong et al. (2003) affirmed these results with model experiments but found a much smaller amplitude in SLP anomalies. However, no significant correlation could be found between autumn snow cover over Siberia and the wintertime SLP or the storm track in the control integration of this model. The impact on the atmospheric circulation is very weak even after extreme snow cover anomalies.

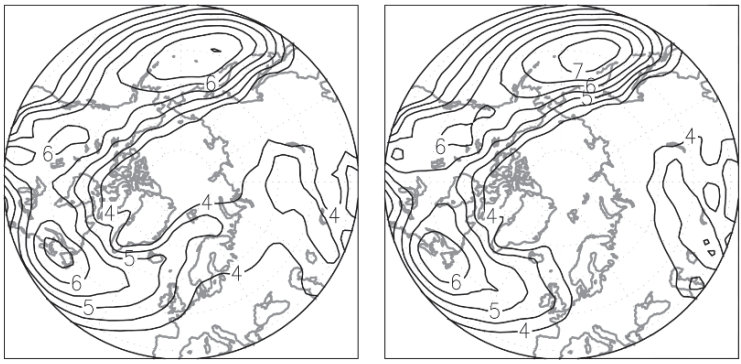

Fig. 8.7 Composite analysis of the standard deviation of the bandpass filtered (2–6-day periods) winter (DJF) daily SLP in hPa for the cases of large positive (left) and negative (right) annual WI1

8.3.3 Role of Sea Ice Thickness for the Export

In the previous sections, the strong influence of the atmospheric circulation on the interannual variability of Fram Strait ice export has been demonstrated. However, studies by Koeberle and Gerdes (2003) and Arfeuille et al. (2000) pointed out that sea ice thickness anomalies have a considerable impact on the export through Fram Strait as well. In both studies, the ice export anomalies have been divided into a part, related to ice thickness anomalies and a part related to ice velocity anomalies. The results indicate an almost equal importance of ice thickness anomalies for the entire export anomalies. Our model results show an increased ice thickness in Fram Strait if the cross-strait SLP-gradient is large. Assuming the same SLP-gradient, sea ice velocity is slightly smaller in Fram Strait with thick ice than with anomalously thin ice. Both, ice velocity and thickness are to large extent driven by the wind. Hence, the results of Koeberle and Gerdes (2003) and Arfeuille et al. (2000) need not to contradict to the high correlation of SLP-gradient and ice export.

To further analyze the relation between ice thickness anomalies in the Arctic and Fram Strait sea ice export, we performed a lag regression analysis (Fig. 8.8). Five

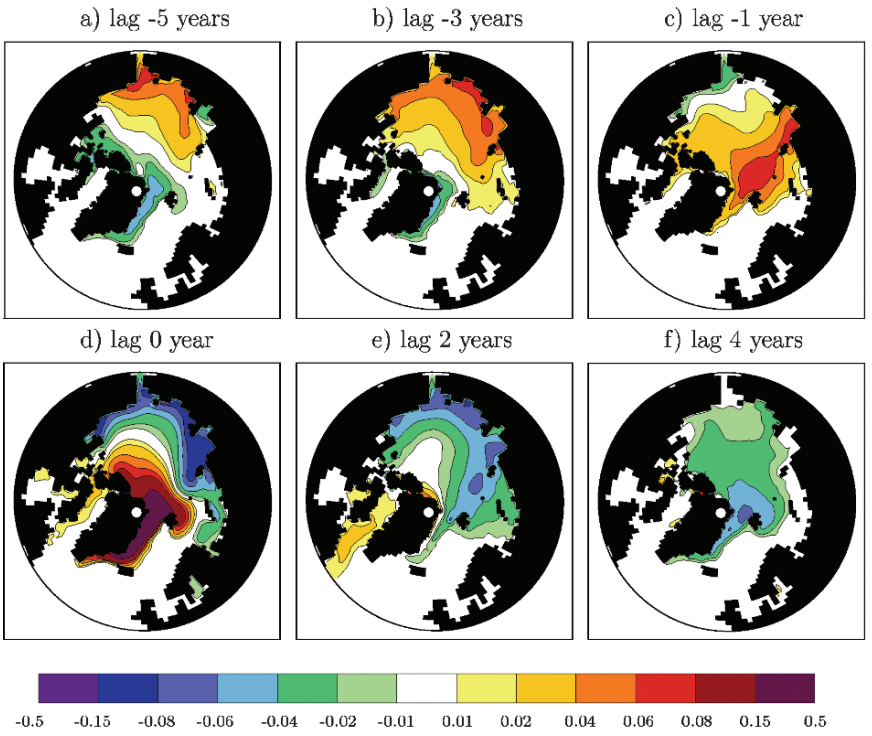

Fig. 8.8 Regression coefficient between annual mean ice exports through Fram Strait and ice thickness anomalies in cm per standard deviation ice export. (a) ice export lags 5 years, (b) ice export lags 3 years, (c) ice export lags 1 year, (d) lag 0, (e) ice export leads 2 years, (f) ice export leads 4 years (Based on Koenigk et al. 2006)

years before high ice exports, positive ice thickness anomalies are formed at the coasts of Chukchi and East Siberian Sea (Fig. 8.8a). In agreement with results by Tremblay and Mysak (1998) and Haak et al. (2003), these anomalies are caused by a convergent ice transport due to an anomalous wind field and are associated with a negative ice export through Fram Strait. In the next 2 years, the positive ice thickness anomaly slowly propagates clockwise along the Siberian coast (Fig. 8.8b) and crosses the Arctic to reach Fram Strait leading the ice export by 1 year (Fig. 8.8c). High ice exports themselves are associated with large anomalous ice transports all across the Arctic towards Fram Strait (Fig. 8.3b) caused by the anomalous atmospheric forcing described above (Fig. 8.3a). A negative ice thickness anomaly occurs at the Siberian coast as a consequence of the divergence in ice transports. It propagates across the Arctic to Fram Strait in the next years, which leads to a decreased ice export (Fig. 8.8e and f) 4 years later. One further year later, the ice export is still reduced and ice thickness at the Siberian coast is again increased. The entire cycle takes about 9 years and matches the peak in the power spectrum of the ice export at the same time scale (Fig. 8.2). A detailed description of this process is given in Koenigk et al. (2006).

This mode has the potential for predictability of the ice export through Fram Strait. Apparently, large ice exports are characterized by previous ice volume anomalies at the Siberian coast and vice versa. Statistical analyses show the largest predictability for the ice export through Fram Strait if ice thickness is increased 2 years before in the Laptev Sea. Figure 8.9 displays the probability distribution of the annual mean ice export 2 years after 69 years with positive and 71 years with negative ice volume anomalies (exceeding the mean ± 1 standard deviation) in the Laptev Sea. After positive anomalies, a considerable shift in the mean ice export towards positive values can be seen and vice versa. The skewness of the distribution is negative after thick ice and positive after previously thin ice in the Laptev Sea. The probability for negative ice export events through Fram Strait is highly

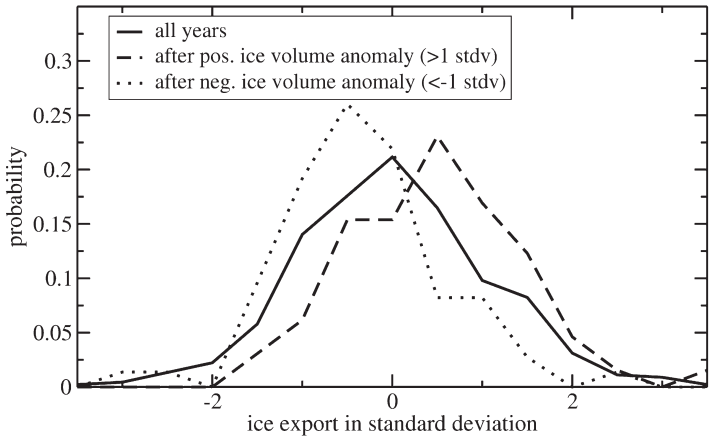

Fig. 8.9 Probability distribution of annual mean Fram Strait ice export 2 years after positive (dashed) and negative ice volume anomalies (dotted) (exceeding one standard deviation) in the Laptev Sea. The solid line gives the mean ice export distribution for all years

decreased while probability for extreme positive events increases only slightly after thick ice in the Laptev Sea.

Ice thickness in the Laptev Sea before extreme ice exports events through Fram Strait, which exceed the mean +2 standard deviations, have been analyzed: In four out of five cases, ice volume has increased by more than one standard deviation 2 years before. All four extreme negative exports have been led by largely reduced ice thickness in the Laptev Sea. The formation of ice thickness anomalies at the coasts of Laptev and East Siberian Sea can be regarded as preconditioning for extreme ice export events through Fram Strait.

8.3.4 Sensitivity Experiment

The Siberian coast is an important source region for the formation of ice volume anomalies. To analyze the propagation of such signals across the Arctic and their interactions with the atmosphere, ice volume anomalies of 2,000 km^3 were prescribed at the Siberian coast in model experiments. Twenty runs were performed, initialized from 1 May of 20 different years with basically normal Fram Strait ice exports. This assures that the initial conditions are not relevant for the ensemble mean. The ice volume anomaly was produced by increasing the ice thickness by 1 m in an area along the Siberian coast and 0.5 m in a transition region (two grid points) to the Central Arctic relative to the initial conditions.

Results of the ensemble mean of these experiments are discussed below. A lag of 1 year is defined as the mean from August in the year in which the experiment starts to July of the following year. Figure 8.10 shows the development of the ice thickness anomaly in the first 3 years after initialization of the experiment. The main part of the anomaly propagates in the transpolar drift stream across the Arctic towards Fram Strait. Already after 1 year, parts of the anomaly reach Fram Strait. After 2 years, the ice anomaly detaches from the Siberian coast and another year later it passes Fram Strait. At the same time, a negative ice thickness anomaly develops at the Siberian coast. This fits well with the regression analysis between Fram Strait ice export and ice thickness (Fig. 8.8).

The ice export through Fram Strait is enhanced in the first 5 years after experiment start with a maximum in the third year. In this period, the anomalous ice export through Fram Strait amounts to two thirds of the imposed sea ice volume anomaly. As the ice export over the Barents Shelf into the North Atlantic is enhanced as well, one can conclude that the Arctic reaches its balance mainly by dynamical reduction of sea ice and subsequent melting in the northern North Atlantic.

Figure 8.11 shows the impact of the imposed ice anomaly after 3 and 4 years. As described above, sea ice export is especially strong after 3 years. This freshwater signal propagates in the East Greenland Current to the south and into the Labrador Sea. Salinity is strongly reduced, which leads to a reduced oceanic convection and more sea ice in the Labrador Sea. Consequently, the oceanic heat release decreases and the air temperature is significantly colder than usual. The SLP responds, especially

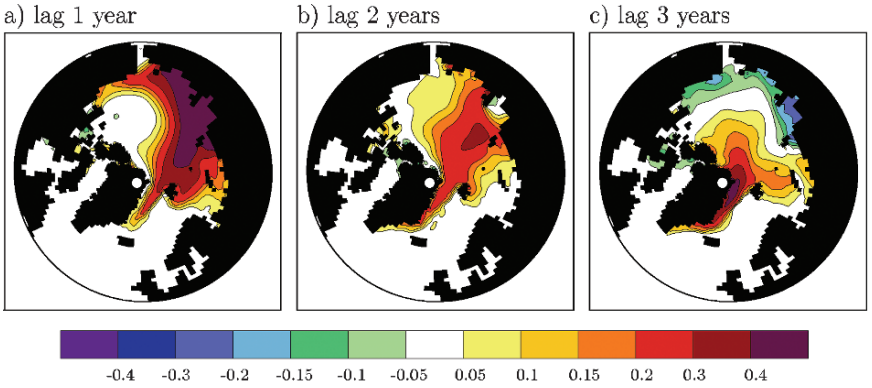

Fig. 8.10 Annual mean sea ice thickness anomalies (in meters) 1–3 years after addition of the ice thickness anomaly at the Siberian coast. Mean of the 20 ensemble runs

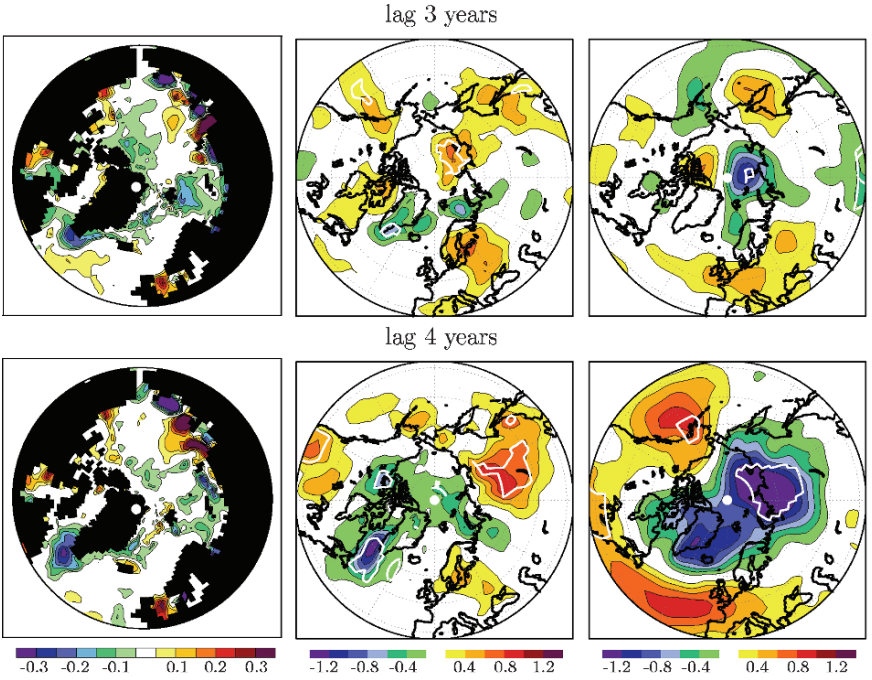

Fig. 8.11 Annual mean anomalies of 10 m salinity (left, psu), 2 m air temperature (middle, Kelvin) and SLP (right, hPa) 3–4 years after addition of the ice thickness anomaly at the Siberian coast. Mean of the 20 ensemble runs. The white lines indicate significance at 95% (for SLP and air temperature, salinity is significant in all colored areas)

in the fourth year, with positive anomalies over the North Atlantic and North Pacific and reduced values further north. This pattern resembles the NAO or AO-pattern. Obviously, the formation process of GSAs can be caused by ice thickness anomalies at the Siberian coast.

In another experiment (detailed description in Koenigk et al. 2006), the effect of extreme export events through Fram Strait has been prescribed. A 3,000 km^3 ice volume anomaly has been implemented in the East Greenland Current south of Fram Strait. Strong and long lasting salinity and temperature anomalies occurred in the Labrador Sea in the following years. Atmospheric circulation responded with a NAO-like pattern 2 years after the mimicked ice export. These results suggest a high skill of predictability after large sea ice exports through Fram Strait.

8.4 Summary and Conclusions

The sea ice export through Fram Strait and its variability have been studied by analyzing a 500-year control integration of a global coupled atmosphere–ocean–sea ice model and by sensitivity studies.

The Fram Strait constitutes the main passage for sea ice out of the Arctic. A comparison of the simulated Fram Strait ice export with observation-based estimates and other model studies has been performed. The estimates of the mean export vary between 70,000 and 100,000 m^3/s, while the spread of the model simulations is slightly larger. Our simulation presents a mean export of 97,000 m^3/s with a standard deviation of 21,000 m^3/s, which also fits well to the observation-based estimates.

Analyses of the variability of the ice export through Fram Strait confirm results of Kwok and Rothrock (1999) that almost 80% of the ice export variability can be explained by the SLP gradient across Fram Strait. In contrast to the NAO, the first planetary-scale zonal SLP wave, meridionally averaged over 70–80° N, is closely related to the ice export through Fram Strait. The phase of the first wave is determined by the position of the extensions of Icelandic Low and Siberian High into the Arctic. According to Cavalieri and Häkkinen (2001), a shift of the phase to the east leads to an increased SLP gradient across Fram Strait in winter. A new index (WI1) combining phase and amplitude of the first planetary wave between 70° and 80° N has been defined in this study. WI1 and ice export are significantly correlated year-round with highest correlation in winter. Moreover, the first zonal wave turned out to be very important for climate variability in the entire Arctic. It is therefore essential to further analyze the processes determining its variability.

The stratospheric polar vortex has been identified as another source of Fram Strait ice export variability. During periods with strong polar vortex, both the SLP gradient across Fram Strait and the ice export are enhanced and vice versa during weak vortex regimes.

In spite of the close relationship between atmospheric forcing and sea ice export through Fram Strait, the atmospheric variability cannot fully explain the 9-year peak in the ice export. This study has presented a sea ice mode on a decadal time scale. It is characterized by the propagation of ice thickness anomalies within the Arctic Basin and leads to decadal ice export variability through Fram Strait. The mechanism of the mode is as follows: onshore winds form an ice thickness anomaly at the coasts of the Siberian and Chukchi Seas. This anomaly

propagates with the mean ice drift along the Siberian coast to the west and crosses the Arctic in the transpolar drift. It reaches Fram Strait 4–5 years after the formation and increases the ice export. The mode develops particularly well if atmospheric forcing strengthens the propagation of the ice anomaly. Simultaneously to the increased ice export, negative ice thickness anomalies occur at the Siberian coast due to offshore winds during high ice exports. They take the same way to Fram Strait in another few years.

In a sensitivity experiment, an ice volume anomaly at the Siberian coast has been prescribed. About two thirds of the prescribed ice volume anomaly are anomalously exported through Fram Strait in the following years. The ice export anomalies provoke the process of GSA-formation in the Labrador Sea, which in turn also affects atmospheric climate conditions. The anomalies in atmospheric circulation force divergent sea ice transports at the Siberian coast, causing anomalously low ice thickness and setting the stage for a negative ice export anomaly through Fram Strait a few years later.

Knowledge of the decadal sea ice mode provides a good framework for predictability. A considerable increase of high ice exports through Fram Strait occurs after previous ice thickness anomalies at the coast of the Laptev Sea. However, the predictability of Labrador Sea climate using the ice export through Fram Strait as predictor seems to be even more promising because the associated processes are less affected by the highly variable atmosphere.

Acknowledgements This work was supported by the Deutsche Forschungsgemeinschaft through the Sonderforschungsbereich 512. The computations have been performed of the Deutsches Klima Rechenzentrum (DKRZ).

References

Aagaard K, Carmack E (1989) The role of sea ice and other fresh water in the Arctic circulation. J Geophys Res 94: 14485–14498

Arfeuille G, Mysak L, Tremblay LB (2000) Simulation of the interannual variability of the wind-driven Arctic sea-ice cover during 1958–1998. Geophys Res Lett 30, doi:10.1029/2002GL016271

Baldwin M, Stephenson D, Thompson D, Dunkerton T, Charlton A, O'Neill A (2003) Stratospheric memory and skill of extended-range weather forecasts. Science 301: 636–640

Belkin I, Levitus S, Antonov J, Malmberg SA (1998) "Great Salinity Anomalies" in the North Atlantic. Progr Oceanogr 41: 1–68

Blackmon M (1976) A climatological spectral study of the 500 mb geoptential height of the Northern Hemisphere. J Atmos Sci 33: 1607–1623

Bojariu R, Gimeno L (2003) Predictability and numerical modeling of the North Atlantic Oscillation. Earth Sci Rev 63 (1–2): 145–168

Brümmer B, Müller G, Affeld B, Gerdes R, Karcher M, Kauker F (2001) Cyclones over Fram Strait: impact on sea ice and variability. Polar Res 20 (2): 147–152

Brümmer B, Müller G, Hober H (2003) A Fram Strait cyclone: Properties and impact on ice drift as measured by aircraft and buoys. J Geophys Res 108 (D7): 6/1–6/13

Castanheira J, Graf HF (2003) North Pacific-North Atlantic relationships under stratospheric control. J Geophys Res 108 (D1): 11/1–11/10

Cavalieri D, Häkkinen S (2001) Arctic climate and atmospheric planetary waves. Geophys Res Lett 28 (5): 791–794
Cavalieri D (2002) A link between Fram Strait sea ice export and atmospheric planetary waves. Geophys Res Lett 29 (12): Art. No. 1614
Christiansen B (2001) Downward propagation of zonal wind anomalies from the stratosphere to the troposphere: Model and reanalysis. J Geophys Res 105: 27307–27322
Cohen J, Saito K, Entkhabi D (2000) The role of the Siberian high in the Northern Hemisphere climate variability. Geophys Res Lett 28 (2): 299–302
Deser C, Walsh J, Timlin M (2000) Arctic sea ice variability in the context of recent atmospheric circulation trends. J Clim 13: 607–633
Deser C, Magnusdottir G, Saravanan R, Phillips A (2004) The effects of North Atlantic SST and sea ice anomalies on the winter circulation in CCM3. Part 2: Direct and indirect components of the response. J Clim 17: 2160–2176
Dickson R, Meincke J, Malmberg SA, Lee A (1988) The "Great Salinity Anomaly" in the northern North Atlantic, 1968–1982. Progr Oceanogr 20: 103–151
Dorn W, Dethloff K, Rinke A, Botzet M (2000) Distinct circulation states of the Arctic atmosphere induced by natural climate variability. J Geophys Res 105 (D24): 29659–29668
Gong G, Entekhabi D, Cohen J (2003) Modeled Northern Hemisphere winter climate response to realistic Siberian snow anomalies. J Clim 16: 3917–3931
Goosse H, Selten F, Haarsma R, Opsteegh J (2002) A mechanism of decadal variability of the sea-ice volume in the Northern Hemisphere. Clim Dyn 19: 61–83
Graversen R, Christiansen B (2003) Downward propagation from the stratosphere to the troposphere: A comparison of two hemispheres. J Geophys Res D24: Art. No. 4780
Haak H, Jungclaus J, Mikolajewicz U, Latif M (2003) Formations and propagation of great salinity anomalies. Geophys Res Lett 30 (9), doi:10.129/2003GL017065
Haak H (2004) Simulation of Low-frequency Climate Variability in the North Atlantic Ocean and the Arctic. Max-Planck-Institute for Meteorology, Reports on Earth System Science, No. 1
Hagemann S, Dümenil L (1998) A parameterisation of the lateral waterflow for the global scale. Clim Dyn 14 (1): 17–31
Hagemann S, Dümenil-Gates L (2003) Improving a subgrid runoff parameterisation scheme for climate models by the use of high resolution data derived from satellite observations. Clim Dyn 21 (3–4): 349–359
Häkkinen S (1993) An Arctic source for the Great Salinity Anomaly: A simulation of the Arctic-ice-ocean system for 1955–1975. J Geophys Res 98 (C9): 16397–16410
Häkkinen S (1999) A simulation of thermohaline effects of a Great Salinity Anomaly. J Clim 6: 1781–1795
Hilmer M, Harder M, Lemke P (1998) Sea ice transport: A highly variable link between Arctic and North Atlantic. Geophys Res Lett 25 (17): 3359–3362
Hilmer M, Jung T (2000) Evidence for a recent change in the link between the North Atlantic Oscillation and Arctic sea ice export. Geophys Res Lett 27 (7): 989–992
Hilmer M, Lemke P (2000) On the decrease of Arctic sea ice volume. Geophys Res Lett 27 (22): 3751–3754
Hurrel J, van Loon H (1997) Decadal variations in climate associated with the North Atlantic Oscillation. Clim Change 36: 301–326
Jung T, Hilmer M (2001) The link between North Atlantic Oscillation and Arctic sea ice export. J Clim 14 (19): 3932–3943
Kalnay E, Kanamitsu M, Kistler R, Collins W, Deaven D, Gandin L, Iredell M, Saha S, White G, Woollen J, Zhu Y, Chelliah M, Ebisuzaki W, Higgins W, Janowiak J, Mo K, Ropelewski C, Wang A, Leetmaa J, Reynolds R, Jenne R, Joseph D (1996) The NCEP/NCAR 40-Year Reanalysis Project. Bull Am Meteor Soc 77 (3): 437–471
Koeberle C, Gerdes R (2003) Mechanisms Determining the Variability of Arctic Sea Ice Conditions and Export. J Clim 16: 2843–2858
Koenigk T, Mikolajewicz U, Haak H, Jungclaus J (2006) Variability of Fram Strait sea ice export: Causes, impacts and feedbacks in a coupled climate model. Clim Dyn 26 (1):17–34, doi: 10.1007/s00382–005–0060–1

Kwok R, Rothrock, DA (1999) Variability of Fram Strait ice flux and North Atlantic Oscillation. J Geophys Res 104 (C3): 5177–5189

Kwok R, Cunningham G, Pang S (2004) Fram Strait sea ice outflow. J Geophys Res 109 (C01009), doi:10.1029/2003JC001785

Latif M, Roeckner E, Botzet M, Esch M, Haak H, Hagemann S, Jungclaus J, Legutke S, Marsland S, Mikolajewicz U, Mitchell J (2004) Reconstructing, monitoring and predicting multidecadal scale changes in the North Atlantic thermohaline circulation with sea surface temperatures. J Clim 17 (5): 857–876

Magnusdottir G, Deser C, Saravanan R (2004) The Effects of North Atlantic SST and Sea Ice Anomalies on the Winter Circulation in CCM3. Part 1: Main features and storm track characteristics of the response. J Clim 17 (5): 857–876

Marsland S, Haak H, Jungclaus J, Latif M, Roeske F (2003) The Max-Planck-Institute global ocean/sea ice model with orthogonal curvilinear coordinates. Ocean Modelling 5: 91–127

Norton W (2002) Sensitivity of Northern Hemsiphere surface climate to simulations of the stratospheric polar vortex. Atmospheric, Oceanic and Planetary Physics, University of Oxford, Oxford, pp. 1–5

O'Hanlon L (2002) Making waves. Nature 415: 360–362

Ostermeier G, Wallace J (2003) Trends in the North Atlantic Oscillation-Northern Annular Mode during the twentieth century. J Clim 16: 336–341

Polyakov I, Johnson M (2000) Arctic decadal and interdecadal variability. Geophys Res Lett 27 (24): 4097–4100

Proshutinsky A, Johnson M (1997) Two circulation regimes of the wind-driven Arctic Ocean. J Geophys Res 102 (C6): 12493–12514

Roeckner E, Bäuml G, Bonaventura L, Brokopf R, Esch M, Giorgetta M, Hagemann S, Kirchner I, Kornblueh L, Manzini E, Rhodin A, Schlese U, Schulzweida U, Tompkins A (2003) The atmosphere general circulation model ECHAM5, part 1: Model description. Max-Planck-Institute for Meteorology, Report No. 349, 127 pp

Schmith T, Hansen C (2003) Fram Strait ice export during the 19th and 20th centuries: Evidence for multidecadal variability. J Clim 16 (16): 2782–2791

Serreze M, Barry R (1988) Synoptic activity in the Arctic Basin, 1979–85. J Clim 1: 1276–1295

Thompson D, Baldwin M, Wallace J (2002) Stratospheric connection to the Northern Hemisphere wintertime weather: Implication for prediction. J Clim 15 (12): 1421–1428

Tremblay L, Mysak L (1998) On the origin and evolution of sea-ice anomalies in the Beaufort-Chukchi Sea. Clim Dyn 14: 451–460

Untersteiner N (1988) On the ice and heat balance in Fram Strait. J Geophys Res 93: 527–531

Valcke S, Coubel A, Declat D, Terray L (2003) OASIS Ocean Atmosphere Sea Ice Soil user's guide. CERFACS, Tech Rep TR/CGMC/03/69, Toulouse, France, 85 pp

Venegas S, Mysak L (2000) Is there a dominant timescale of natural climate variability in the Arctic? J Clim 13: 3412–3434

Vinje T (2001) Fram Strait ice fluxes and atmospheric circulation: 1950–2000. J Clim 14: 3508–3517

Vinje T, Finnekåsa O (1986) The ice transport through the Fram Strait. Norsk Polarinst. Skrifter 186: 1–39

Vinje T, Nordlund N, Kvambeck A (1998) Monitoring the ice thickness in Fram Strait. J Geophys Res 103: 10437–10449

Walsh J, Chapman W (1990) Arctic contribution to upper ocean variability in the North Atlantic. J Clim 3 (12): 1462–1473